Response Variability and Timing Precision of Neuronal Spike Trains *In Vivo*

Daniel S. Reich[1,2], Jonathan D. Victor[1,2], Bruce W. Knight[1], Tsuyoshi Ozaki[1], and Ehud Kaplan[1,3]

December 11, 1996

[1]Laboratory of Biophysics, The Rockefeller University, 1230 York Avenue, New York, NY 10021

[2]Department of Neurology and Neuroscience, Cornell University Medical College, 1300 York Avenue, New York, NY 10021

[3]Current address: Department of Ophthalmology, Mt. Sinai School of Medicine, New York, NY 10029

Address correspondence to:
Ehud Kaplan
Department of Ophthalmology
Mt. Sinai School of Medicine
1 Gustave Levy Place
New York, NY 10029
Tel: 212-241-9607
Fax: 212-289-5945
E-mail: kaplane@rockvax.rockefeller.edu

Special abbreviations used in this paper:

CRT	*cathode ray tube*
IPS	*impulses per second*
LGN	*lateral geniculate nucleus*
PSTH	*peri-stimulus time histogram*

SUMMARY AND CONCLUSIONS

We report that neuronal spike trains can exhibit high, stimulus-dependent temporal precision even while the trial-to-trial response variability, measured in several traditional ways, remains substantially independent of the stimulus. We show that retinal ganglion cells and neurons in the lateral geniculate nucleus (LGN) of cats *in vivo* display both of these aspects of firing behavior, which have previously been reported to be contradictory. We develop a simple model which treats neurons as "leaky" integrate-and-fire devices and show that it, too, can exhibit both behaviors. We consider the implications of our findings for the problem of neural coding.

Introduction

The variability of neurons' response patterns has been studied extensively and is widely considered to be large (see Shadlen and Newsome 1994 for a review). For retinal ganglion cells in intact mammals, one particular measure of trial-to-trial variability—the standard deviation of the cell's responses to multiple cycles of a sinusoidal grating—is consistently independent of all of the following: contrast; region (center or surround) or fraction of the receptive field stimulated; and overall illumination (Croner *et. al.* 1993; Reich *et. al.* 1994). On the other hand, retinal ganglion cells in rabbit and salamander respond with high temporal precision to a flickering full-field light stimulus (Berry *et. al.* 1996), as do cells in rat neocortical slices that are directly injected with time-varying current (though these cells respond much less precisely to steady stimulation; Mainen and Sejnowski 1995). Indeed, based on their results, Mainen and Sejnowski suggest that the "intrinsic noise" of neurons is low. Moreover, even in the so-called "higher areas" of the visual cortex of awake monkeys, neurons can respond to visual stimuli by firing spikes at the same times in every stimulus presentation (Bair and Koch 1996). Nonetheless, there continues to be substantial debate regarding the size of variability at the various levels of the mammalian visual system (Softky and Koch 1993; Gur *et. al.* 1996).

While these widely divergent reports of the size and nature of neuronal variability may seem to be inherently paradoxical, they are not. We show here that neurons *in vivo* routinely exhibit, in the same spike trains, both high, stimulus-dependent temporal precision and, simultaneously, stimulus-independent variability among repeated responses to a given stimulus, even while the response itself changes dramatically. This behavior was found in every cell examined in our study. A simple theoretical model for neuronal firing—the "leaky" or "forgetful" integrator (Knight 1972)—also produces this sort of spiking behavior and provides a straightforward resolution of the apparent paradox.

Methods

Experiments. We recorded extracellularly the activity of lateral geniculate nucleus (LGN) neurons and their retinal inputs in anesthetized, paralyzed cats (Kaplan *et. al.* 1987). Briefly, experiments were performed on adult cats, two males and one female. The behavior described in this paper was seen in all four cells from which recordings suitable for this type of analysis were made. Anesthesia was induced by intramuscular injections of xylazine (1 mg/kg) and ketamine (10 mg/kg) and was maintained during surgery and recording with intravenous injections of thiopental (2.5%, 2-6 mg/kg/hr). Paralysis was induced and maintained with vecuronium (0.25 mg/kg/hr) or pancuronium (0.3-0.5 mg/kg/hr). Gas-permeable hard contact lenses were used to prevent corneal drying, and artificial pupils (3 mm diameter) were placed in front of the eyes. Blood pressure, heart rate, and expired CO_2 were continuously maintained within the physiological range. The optical quality of the animal's eyes was checked regularly by ophthalmoscopy. Our experimental protocol was approved by the Rockefeller University Animal Care and Use Committee and was in accordance with the NIH guidelines for the use of higher mammals in neuroscience experiments.

A tungsten-in-glass electrode (5-10 μ tip) recorded spikes from a single LGN neuron and from its retinal ganglion cell input in the form of extracellular synaptic (S) potentials (Bishop *et. al.* 1958). The electrode signal was amplified and monitored conventionally. Visual stimuli were created on a white CRT (Conrac, 135 frames/s, 100 cd/m^2 mean luminance) by specialized equipment developed in our laboratory. The eyes were refracted to focus at the viewing distance of 114 cm. LGN spikes and S potentials were timed to the nearest 0.1 ms.

Model. The model we used is based on the evolution of a dimensionless state variable whose value, compared to a stochastic firing threshold, determines when the cell fires (Knight 1972). The state variable evolves by $V(t) = \int_0^t f(t) e^{-(t-t')/\tau} dt'$, where t is the time since the previous spike, τ is the time constant of the leak, and $f(t) = \max\{A_0 + A_1 \cos(\omega t + \varphi), 0\}$ is the sinusoidally-modulated input. This model is a limiting case of the Hodgkin-Huxley equations for neuronal firing (Knight 1972), and the state variable $V(t)$ plays the role of the intracellular voltage. $V(t)$ is recalculated every 0.1 ms. The cell fires when $V(t)$ reaches a threshold whose value is chosen randomly from a uniform distribution (in our simulation, between 0.7 and 0.9); a new threshold is calculated after each spike is fired. (Versions of the simulation in which the threshold changes every 0.1 ms, or in which the probability of firing increases exponentially as the state variable nears the threshold, yield similar results.) The single parameter that was varied in this study was A_1, the amplitude of the sinusoidal stimulus. The constant parameters were: A_0 = 50.0 IPS; $\omega/2\pi$ = 4 Hz; $\varphi = \pi$; τ = 20 ms. The first few stimulus cycles were discarded to ensure steady-state behavior of the model.

Analysis. We calculated (1) high-resolution (1 ms bins) peri-stimulus time histograms, representing the binned nerve impulses in response to multiple presentations of the same stimulus, to show the firing rate at any time during the response cycle; and (2) mean rates and stimulus-locked Fourier fundamental components of these response records to evaluate the amplitude and variability of the neuron's response. Three separate measures of response variability were calculated: (1) the vector standard deviation of the single-cycle Fourier fundamental component (Croner *et. al.* 1993), which is the square root of the sum of the variances of the real and imaginary parts of the Fourier components, taken separately; (2) the standard deviation of the single-cycle Fourier fundamental amplitudes (a phase-independent measure which is always smaller than the amplitude-and-phase measure, calculated above); and (3) the standard deviation of the spike count in each trial (also known as the mean rate variability).

Results

Fig. 1 shows the peri-stimulus time histogram (PSTH) of an LGN neuron's response to 1024 cycles of a drifting 4 Hz sinusoidal grating, presented at three different contrasts (0%, 32%, and 100%). There are no preferred times for spikes to occur in the unmodulated (0%) case. At 32% contrast, the first spike in each response tends to be fired at a reliable and reproducible time (the large peak), but later spikes are more widely distributed (Fig. 1B). At 100% contrast, however, there are several large but narrow peaks in the PSTH that occur after the initial spike (Fig. 1C). As a measure of temporal precision akin to that used by other investigators (Mainen and

Sejnowski 1995), we fit each peak in the PSTH to a Gaussian distribution and measured the width of each distribution in the 100% contrast situation. By this measure, the temporal precision for the first few spikes of this cell's response was on the order of ±5 ms. Fig. 1D is a raster plot of all the spike times for the responses whose PSTH is shown in Fig. 1C. The slow drift seen in the rasters indicates that our measure of precision is conservative, and the small, gradual change in response pattern that occurs through trial number 250 could be due to a change in eye position. For the sake of completeness, we have shown the responses to all 1024 cycles of the stimulus.

Similar behavior is found in retinal ganglion cells. Fig. 2A shows the PSTH of the response of an X-type, ON-center retinal ganglion cell to 1024 cycles of a 4 Hz drifting grating at 32% and 100% contrast. Also shown is a plot of response *vs*. contrast (on a semilogarithmic scale), which demonstrates that, while the response amplitude increases significantly with contrast, the three measures of response variability (see above) remain relatively constant. Preferred firing times are again evident in the 100% case, with a precision of approximately ±5 ms for the first few spikes; we show one of the Gaussian distributions used to measure this timing precision. Thus, response variability (measured in any of the three ways shown in the figure) is independent of whether spikes are precisely timed (in the high-contrast regime) or not (in the low-contrast regime).

Fig. 2B shows the response of an X-type, OFF-center cell to the same stimulus. The temporal precision is on the order of ±3 ms. Note that the response variability for this cell is not constant over low contrasts; that is because this OFF cell fires very few spikes at low contrast. However, once the mean rate exceeds 3 impulses per second (IPS) at 2% contrast, the response variability reaches its maximum value and remains flat thereafter, even while the firing precision (and mean firing rate) increases dramatically. Thus, despite the differences from the ON-center cell at low contrasts, the data from this cell support our conclusion that response variability is stimulus-independent while firing precision is stimulus-dependent, at least over a reasonable range of contrasts.

Fourier analysis reveals that the precise spike timing is not an artifact of the frame rate (135 Hz) of the stimulating CRT. For the data presented in Fig. 1C, for example, the nearest peaks in the power spectrum of the spike train occur at 121 and 140 Hz; for the data in Fig. 2A there is a small peak at 90 Hz; and for the data in Fig. 2B, the nearest peaks are at 120 and 145 Hz. Moreover, the interpeak intervals vary throughout the response cycle.

We show now that a simple model—namely, a "leaky" integrate-and-fire neuron with a stochastic threshold, which fires in response to sufficient input but which forgets its previous input at an exponential rate—robustly exhibits, in the same response discharge, high, stimulus-dependent temporal firing precision together with stimulus-independent response variability. The key parameter of the model is the rate at which the neuron forgets its previous input. Responses to strongly-modulated stimuli typically include a period of intense firing alternating with a quiet period when no spikes are fired, i.e., when the model cell is relatively inhibited. If the time constant of the leak (a stimulus-independent parameter) is shorter than the quiet period (a stimulus-dependent response property), the neuron "forgets" the residual input that is integrated during the active portion of the response. Therefore, the neuron's initial state is restored after the inactive period of every stimulus cycle at high modulation depth, and response fluctuations do not accumulate from cycle to cycle.

Fig. 3A shows PSTHs of the model's response to 1024 cycles of a 4 Hz sinusoidal grating at 0%, 16%, and 100% contrast. Although the range of variation of the stochastic threshold is the same in all three cases, the firing precision is high at high contrast and low at lower contrasts. Fig. 3B plots the model's response *vs*. contrast, showing that all measures of response variability are independent of contrast, while the response amplitude, measured as the Fourier fundamental or the mean rate, generally increases with contrast.

Note that at 100% contrast, the firing precision is lower for spikes that occur later in the response cycle, as the width of the histogram's sharp peaks increases with time. This is because errors in absolute spike time (due to the stochastic threshold) accumulate as successive spikes are fired during each response cycle. Fig. 3C shows the probability distribution of the internal state variable of the model (which resets to zero after each spike is fired) at three different times during the stimulus cycle (50, 75, and 190 ms), all at 100% contrast. At 50 ms, before any spikes have been fired, the distribution is very narrow because there has been no opportunity for variability to accumulate. Because of the model's stochastic threshold, the first spike in each trial occurs at a slightly different time (the first peak in the 100% contrast histogram in Fig. 3A is narrow but has a nonzero width). Each spike causes the state variable to reset to zero, so the amount of input that has accumulated by 75 ms varies depending on when the first spike was actually fired. This accounts for the wider distribution at 75 ms. The distribution of the state variable at an intermediate time (say, 65 ms, in the middle of the first peak of the histogram) is bimodal, since on some trials the cell has already fired and the state variable is near zero, while on others the cell has not yet fired and the state variable is near threshold. At 190 ms, after all the spikes have occurred, the distribution of the state variable is wider than at 50 or 75 ms, since a great deal of variability has accumulated after many spikes have fired. The difference in the width of the distribution between 75 ms and 190 ms is sufficient to account for the precise firing of the first few spikes in each response and the imprecise firing of the last few.

Note that either a stochastic threshold or additive (stimulus-independent) background noise in the cell's membrane potential is sufficient to ensure that the model does not respond identically to every presentation of the stimulus. Both of these types of input noise yield qualitatively similar PSTHs. In fact, our rather abstract model with a fluctuating firing threshold, and the more physiologically realistic model in which the noise is introduced by a stimulus-independent fluctuating input current, are very closely related. Imagine a simulation in which we followed the state variable from one spike to the next in the absence of the fluctuating input current and then followed it in a large sample of cases with the noisy current present. At the moment that each noisy run crosses threshold, subtract from the state variable the value it had at that moment in the noise-free run. Our collection of differences has a probability distribution which can be regarded as an equivalent distribution of threshold values for the stochastic-threshold case, and will yield an identical distribution of interspike-interval values for that spike pair. If the noise does not dominate the result, then, the two kinds of systems have the same response characteristics. However, the actual distribution of the state variable at any time is different (i.e., the state variable has intrinsic variability which is reflected in its distribution even before the first spike is fired).

Discussion

Our results indicate that analyzing the size and nature of neuronal variability is not straightforward—that several measures of variability must be considered. For example, we consider the response variability, measured as the standard deviation of the fundamental Fourier components for each response cycle (considering or disregarding the phase of the response) and as the standard deviation of the spike count in each cycle, as well as the variability of timing of individual spikes. It is not obvious that there is any simple relationship among these various measures of variability.

These two general types of variability—one which is substantially independent of the stimulus and the other strongly dependent on the stimulus—can both be generated by a single process: background noise that affects the neuron's membrane potential, or, equivalently, fluctuations in the firing threshold. This noise could come, for example, from the barrage of excitatory and inhibitory inputs that converge on many cells in the brain (Shadlen and Newsome 1994). In our model, all the various potential sources of neuronal noise are included in a single parameter, the fluctuation in the firing threshold of the model cell.

The firing precision we report here is lower than that recently reported for neurons in a rat neocortical slice (Mainen and Sejnowski 1995). This is not surprising: our experiments were performed *in vivo*, where synaptic activity is higher, and in a different region of the brain; in addition, our stimuli were delivered through the natural neural pathway, in which variability could accumulate at each of several stages. Moreover, the firing precision we found is on the same order of magnitude as that reported in the retinae of salamanders and rabbits (Berry *et. al.* 1996) and even in area MT of awake monkeys (Bair and Koch 1996).

Several investigators have proposed that the timing of individual spikes, and not merely the mean firing rate or the Fourier fundamental, carries information that is accessible to the nervous system (Bullock 1968; Richmond *et. al.* 1987; Bialek *et. al.* 1991; Abeles *et. al.* 1994; Hopfield 1995; Softky 1995; Victor and Purpura 1996). Our data do not provide information about which response measure the neuron uses, or about which source of variability plays a greater role in information processing in the brain. However, our demonstration that visual neurons stimulated at high contrast can fire with high temporal precision, while the same neurons stimulated at lower contrasts do not, raises the question of whether this phenomenon occurs only under extreme conditions, or whether it is present, albeit less obviously, in responses to weaker stimuli. A finding that spike timing is important for responses to weakly-modulated stimuli (not reported here) would suggest that the nervous system can extract timing information from a blur of different spike times—that it could distinguish spikes that provide information about the stimulus from those that are due to noise and that therefore fall at the "wrong" time. Such an algorithm could involve, for example, comparing the timing of spikes in several neurons which carry similar information. Alternatively, the mode of information transmission may switch from detection (in a regime in which spike times are imprecise and timing is not used to convey information) to discrimination (in a regime in which spike times are precise).

REFERENCES

Abeles, M., Prut, Y., Bergman, H., and Vaadia, E. Synchronization in neuronal transmission and its importance for information processing. *Prog. Brain Res.* **102**:395-404, 1994.

Bair, W. and Koch, C. Temporal precision of spike trains in extrastriate cortex of the behaving macaque monkey. *Neural Comput.* **8**:1185-1202, 1996.

Berry, M.J., Warland, D.K., and Meister, M. The precision of retinal spike trains. *Soc. Neurosc. Abstr.* **22**:493, 1996.

Bialek, W., Rieke, F., de Ruyter van Steveninck, R., and Warland, D. Reading a neural code. *Science* **252**:1854-1857, 1991.

Bishop, P.O., Burke, W., and Davis, R. Synapse discharge by single fibre in mammalian visual system. *Nature* **182**:728-730, 1958.

Bullock, T.H. Representation of information in neurons and sites for molecular participation. *Proc. Natl. Acad. Sci. U.S.A.* **60**:1058-1068, 1968.

Croner, L.J., Purpura, K., and Kaplan, E. Response variability in retinal ganglion cells of primates. *Proc. Natl. Acad. Sci. U.S.A.* **90**:8128-8130, 1993.

Gur, M., Beylin, A., and Snodderly, D.M. Response variability of cells in V1 of alert monkeys is low. *Soc. Neurosc. Abstr.* **22**:283, 1996.

Hopfield, J.J. Pattern recognition computation using action potential timing for stimulus representation. *Nature* **376**:33-36, 1995.

Kaplan, E., Purpura, K., and Shapley, R.M. Contrast affects the transmission of visual information through the mammalian lateral geniculate nucleus. *J. Physiol.* **391**:287-288, 1987.

Knight, B.W. Dynamics of encoding in a population of neurons. *J. Gen. Physol.* **59**:734-766, 1972.

Mainen, Z.F. and Sejnowski, T.J. Reliability of spike timing in neocortical neurons. *Science* **268**:1503-1506, 1995.

Reich, D.S., Sanchez-Vives, M., Mukherjee, P., and Kaplan, E. Response variability of retinal ganglion cells is independent of the synaptic pathway activated and of retinal illumination. *Invest. Ophth. Vis. Sci.* **35** (suppl.):4032, 1994.

Richmond, B.J., Optican, L.M., Podell, M. & Spitzer, H. Temporal encoding of two-dimensional patterns by single units in primate inferior temporal cortex. I. Response characteristics. *J.Neurophysiol.* **57**:132-146, 1987.

Shadlen, M.N. and Newsome, W.T. Noise, neural codes and cortical organization. *Curr. Opin. Neurobiol.* **4**:569-579, 1994.

Softky, W.R. and Koch, C. The highly irregular firing of cortical cells is inconsistent with temporal integration of random EPSPs. *J. Neurosci.* **13**:334-350, 1993.

Softky, W.R. Simple codes versus efficient codes. *Curr. Opin. Neurobiol.* **5**:239-247, 1995.

Victor, J.D. and Purpura, K. Nature and precision of temporal coding in visual cortex: a metric-space analysis. *J. Neurophysiol.* **76**:1310-1326, 1996.

ACKNOWLEDGMENTS

We thank Dan Samber and Pratik Mukherjee for technical and scientific assistance, and Liat Kaplan for reading the manuscript. This research was supported by grants EY4888, EY1428, EY9314, MH50166, and ONR N0014-93-12079. DSR was supported by an MSTP grant awarded by Cornell University Medical College and The Rockefeller University, as well as by a SURF fellowship from The Rockefeller University. EK is Jules and Doris Stein *Research to Prevent Blindness* Professor at The Mount Sinai School of Medicine.

FIGURE LEGENDS

Figure 1. Neurons *in vivo* can fire action potentials at precise, reproducible times. Peri-stimulus time histograms (PSTHs) from an X-type, ON-center cell in the cat lateral geniculate nucleus for 1024 cycles of a 4 Hz, 0.15 cycles/degree, drifting sinusoidal grating. The vertical axis represents the firing rate in impulses per second (IPS) in each 1 ms bin. (**A**) 0% contrast. (**B**) 32% contrast. (**C**) 100% contrast. Note that the vertical scale in (A) is 10 times greater than in (B) and (C). (**D**) Raster plot of the data from (C), showing that the cell's response is relatively stationary across response cycles.

Figure 2. Spike timing can be precise even while response variability is substantial. (**A**) X-type, ON-center retinal ganglion cell recorded as S-potentials in the cat LGN. The stimulus was a drifting grating (4 Hz, 1.2 cycles/degree, 1024 cycles). PSTHs are shown for the responses to stimuli at 32% and 100% contrast. Again, the vertical axis shows the firing rate in each 1 ms bin. The bottom plot shows the cell's response *vs*. contrast, on a semilogarithmic scale. Five data points are plotted for each contrast: the mean firing rate (filled circles); the amplitude of the mean Fourier fundamental (filled squares); the variability of the mean rate (open circles); the variability of the Fourier fundamentals (open squares); and the phase-independent variability of the Fourier fundamentals (squares with a dot in the center). (**B**) As in (A), but here the cell is an X-type, OFF-center retinal ganglion cell stimulated with a drifting grating at 32% and 100% contrast (4 Hz, 1.05 cycles/degree, 1024 cycles). Note that the cell exhibited a 1 to 2 minute period of nonstationary firing (obvious in the raster diagrams, which are not shown here) during two of the stimulus conditions (4% and 16% contrast); this corresponded to roughly 250 to 500 cycles of the 4 Hz stimulus. Including these trials in the response and response variability calculations yielded unexpectedly high values at those two contrasts; however, deleting those trials at the two contrasts (and analyzing the 750 to 1000 remaining ones) resulted in values that clearly followed the trend for the eight other contrasts we tested. We plot the data analyzed without the "variant" firing for the sake of clarity.

Figure 3. A "leaky," or "forgetful," integrate-and-fire model, with noise added to its firing threshold, simultaneously displays high timing precision and substantial response variability. (**A**) PSTHs of the model's response to 1024 presentations of a 4 Hz sinusoidal stimulus at 0%, 16%, and 100% contrast. The arrows at 50, 75, and 190 ms in the 100% panel indicate the times for which the state variable's distribution is shown in (C). (**B**) The model's response *vs.* contrast. (**C**) The probability distribution of the model's state variable, akin to the membrane potential of a real neuron, at three times during the cycle, in response to stimulation at 100% contrast. See text for details.

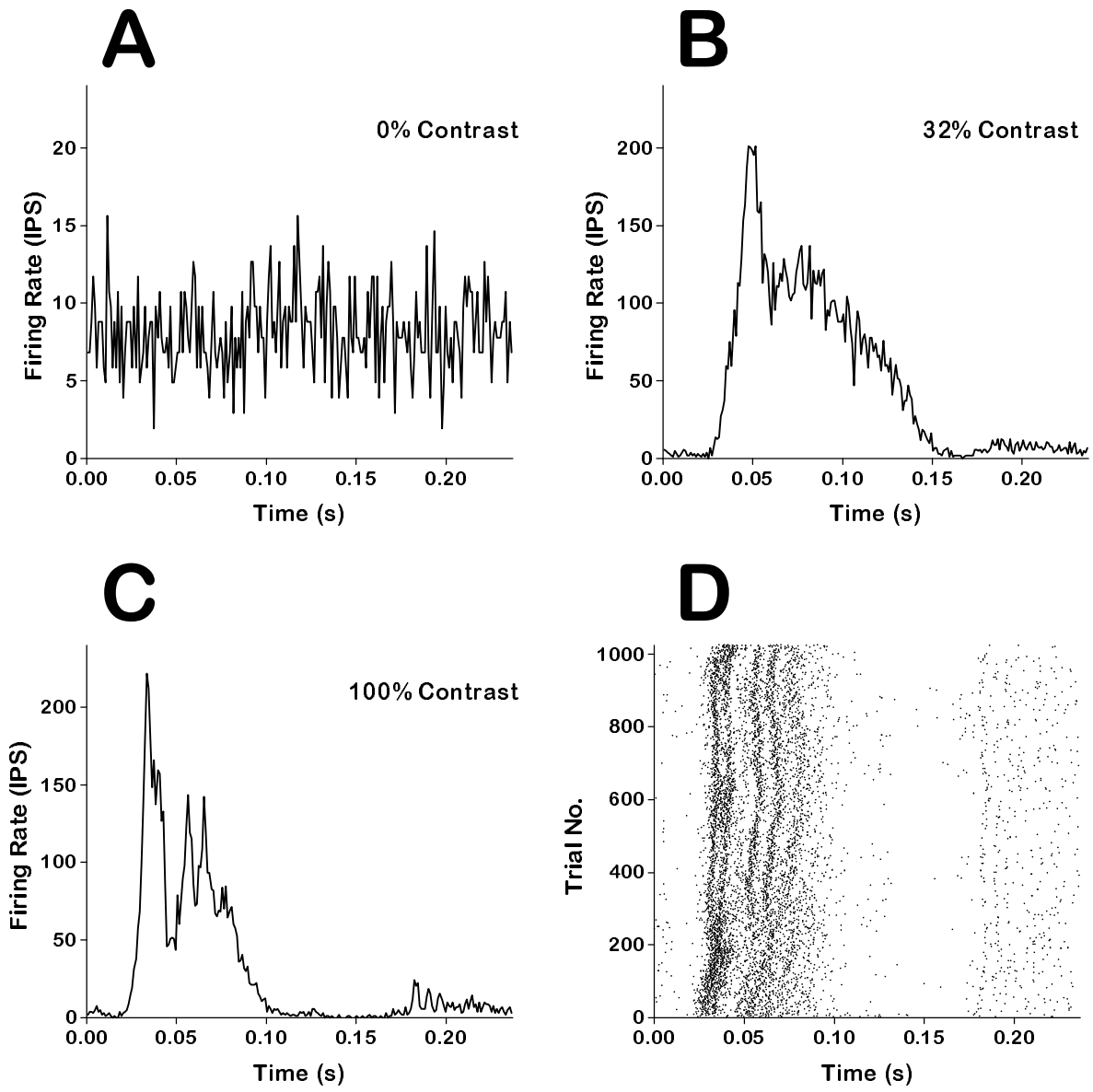
A
0% Contrast
Firing Rate (IPS)
Time (s)
B
32% Contrast
Firing Rate (IPS)
Time (s)
C
100% Contrast
Firing Rate (IPS)
Time (s)
D
Trial No.
Time (s)

Fig. 1

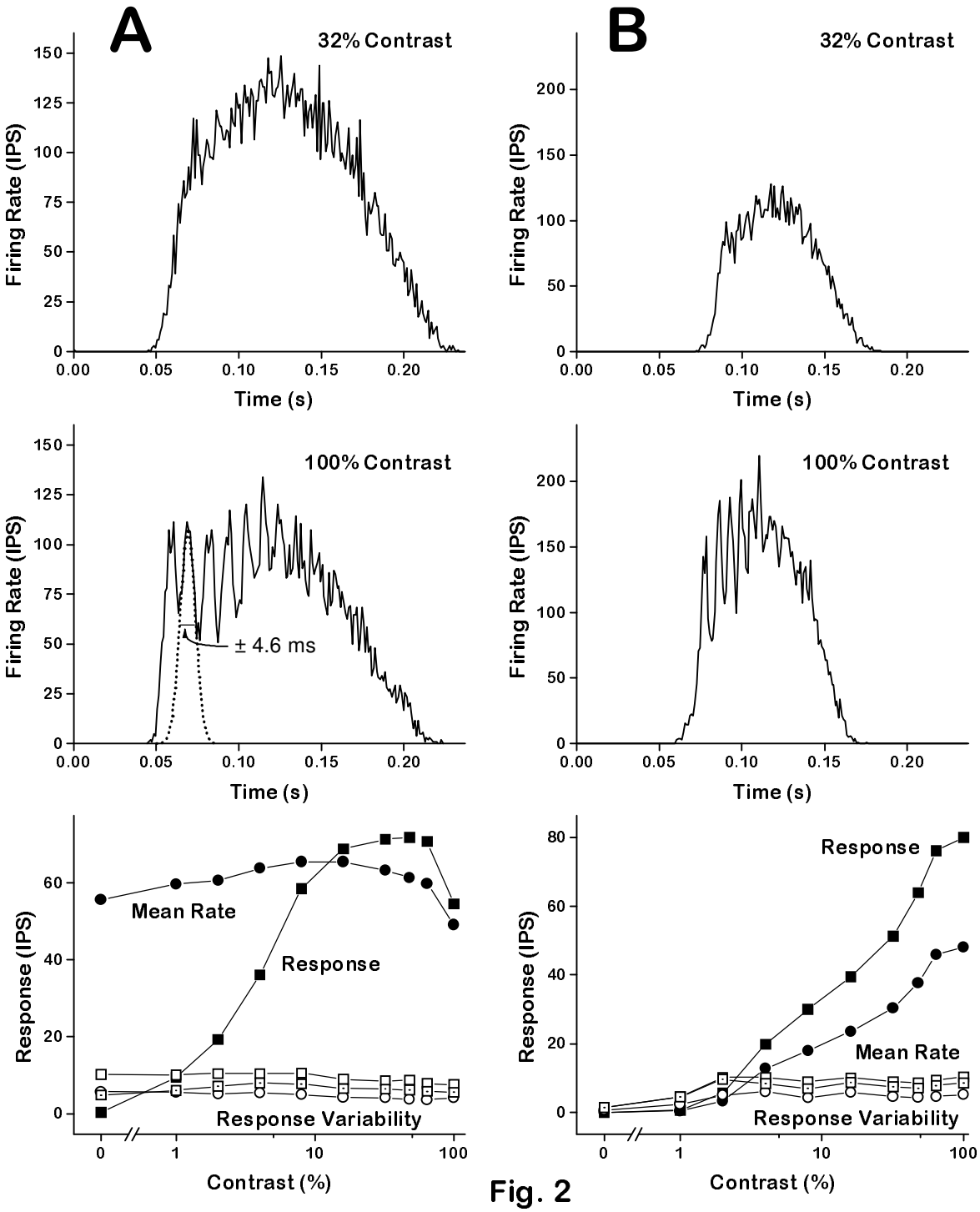
A
32% Contrast
Firing Rate (IPS)
Time (s)
B
32% Contrast
Firing Rate (IPS)
Time (s)
100% Contrast
± 4.6 ms
Firing Rate (IPS)
Time (s)
100% Contrast
Firing Rate (IPS)
Time (s)
Mean Rate
Response
Response Variability
Response (IPS)
Contrast (%)
Response
Mean Rate
Response Variability
Response (IPS)
Contrast (%)

Fig. 2

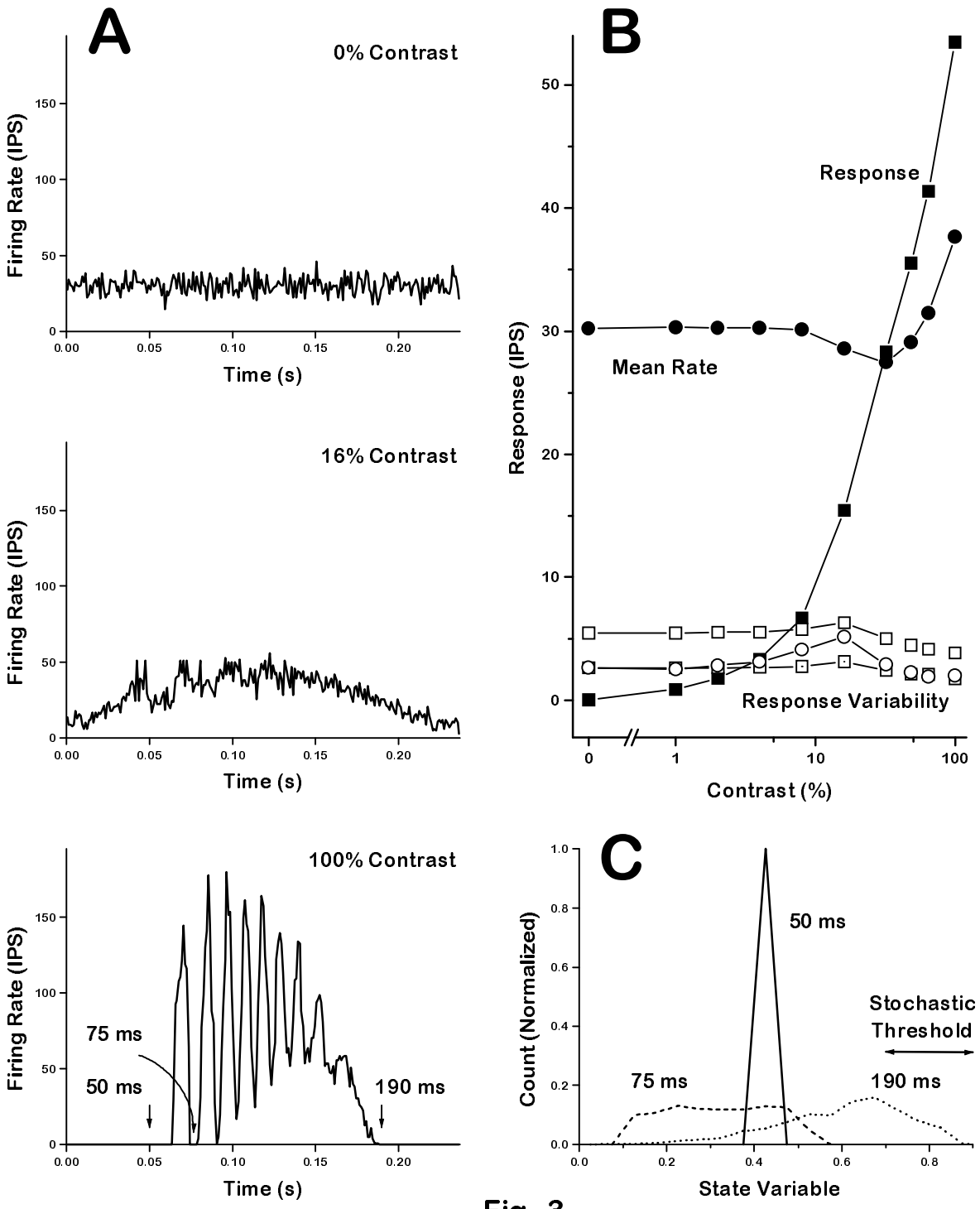
A
0% Contrast
Firing Rate (IPS)
Time (s)
16% Contrast
100% Contrast
75 ms
50 ms
190 ms
B
Response
Mean Rate
Response Variability
Response (IPS)
Contrast (%)
C
50 ms
75 ms
190 ms
Stochastic Threshold
Count (Normalized)
State Variable

Fig. 3